2021 IEEE 18th International Symposium on Biomedical Imaging (ISBI)
April 13-16, 2021, Nice, France

2021 IEEE 18th International Symposium on Biomedical Imaging (ISBI) | 978-1-6654-1246-9/20/$31.00 ©2021 IEEE | DOI: 10.1109/ISBI48211.2021.9434060

MASSIVE-TRAINING ARTIFICIAL NEURAL NETWORK (MTANN) WITH SPECIAL KERNEL FOR ARTIFACT REDUCTION IN FAST-ACQUISITION MRI OF THE KNEE

Maodong Xiang[1,2], Ze Jin[1,2], Kenji Suzuki[1,2]

[1]Department of Information and Communications Engineering, School of Engineering, Tokyo Institute of Technology
[2]Laboratory for Future Interdisciplinary Research of Science and Technology, Institute of Innovative Research, Tokyo Institute of Technology

ABSTRACT

Accelerated MRI acquisitions by taking fewer samples in the k-space involve a trade-off between the image-quality degradation due to artifacts and acquisition time. The purpose of our study was to reduce artifacts in reconstructing MR images from under-sampled k-space data in fast-acquisition MRI. In this study, we proposed a novel massive-training artificial neural network (MTANN) scheme coupled with a k-space-sampling-pattern-specific kernel to improve the image quality by reducing artifacts while preserving the anatomic structures. We conducted experiments to evaluate the performance of our scheme with under-sampled MR images of 20 patients with 795 slices. The results showed that our proposed MTANN scheme reduced artifacts in reconstructed MR images from under-sampled k-space data substantially, while the image quality was well-maintained.

Index Terms— Deep learning, truncation artifact, under-sampled MRI, image processing, sparse data

1. INTRODUCTION

Magnetic resonance imaging (MRI) is a non-invasive diagnostic modality that images the anatomy structures of patients for the diagnosis of a range of diseases. However, MRI has a serious disadvantage of a long acquisition time, resulting in a low throughput, patient discomfort, motion artifacts, and a high exam cost [1], [2].

When a frequency-encoding gradient is applied during the scan process, the k-space (frequency domain) data are taken directly from the MR signal [3]. One common approach to accelerate MRI data acquisition is to take fewer measurements in the k-space, obtaining under-sampled k-space data. Such accelerated MRI acquisitions involve a trade-off between image quality degradation mainly caused by the truncation artifacts due to the limited k-space data and acquisition time. In theory, an image can be represented as a summation of sine waves of different amplitudes, phases, and frequencies. However, an accelerated scan with fewer MR signals results in lacks of specific harmonics in the Fourier series, which creates truncation artifacts in the reconstructed MR image. A truncation artifact consists of multiple rings of a regular periodicity occurring at abrupt transitions in signal intensity [4]. There are several choices of trajectories in the data acquisition in two dimensions, such as radial and spiral sampling patterns, but the most commonly used one in MRI machines today consists of straight lines known as the Cartesian grid [5].

Compressed sensing has been applied for improving the quality of MR images reconstructed from under-sampled k-space data in current MR machines. In compressed sensing methods, the identification of the optimal sparse transform often plays an essential role. Those sparse transformations are often designed by considering some prior information such as wavelet transform and total variation (TV) [6]. However, compressed sensing methods are usually iterative solutions and take a long computational time. Besides, it is often challenging to set hyperparameters that control a balance between the preservation of image details and the removal of artifacts [7], [8].

Recently, deep learning methods are being used in medical imaging [9], such as image quality improvement in CT [10], mammography [11], and tomosynthesis [12]. However, it is a great challenge for current deep learning methods to recover high-frequency details and remove truncation artifacts in the under-sampled MR images simultaneously, especially with a high acceleration factor [13]. Additionally, most of the deep learning methods did not take the theoretical nature of the under-sampling process in the k-space into consideration [13], [14], [15], [16].

In this paper, we applied a massive-training artificial neural network (MTANN) deep-learning method coupled with a k-space-sampling-pattern-specific kernel to improve the image quality by reducing artifacts while preserving the anatomic structures in MR images reconstructed from under-sampled MR data. We conducted experiments on knee MR images to show the advantages and limitations of the proposed method over a traditional compressed sensing method [6].

2. METHODS AND MATERIALS

2.1. Knee MRI database

The database used in this study contains 795 raw k-space images of the knee MRI from 20 patients. All data were acquired using a clinical 3T MRI system (Siemens Magnetom Skyra, Siemens Medical Solutions, Erlangen, Germany) [15]. The age of the 20 patients ranges from 15 to 76 years. Each knee reconstructed MR image has an in-plane matrix size of 320 x 320 pixels, with a resolution of 0.44 x 0.44 mm^2. The slice thickness of each slice is 4.5 mm, with a spacing between slices of 3 mm. As the original data were in the k-space, the Fourier transform was applied to the k-space data to reconstruct fully-sampled MR images. The under-sampling was performed by selecting a specific number of acquisition lines in the MR phase encoding direction from the fully-sampled k-space data to simulate the fast acquisition MR process. 20% around the central low frequency were preserved; and top 5% high frequency lines were selected according to the k-space energy distribution of the dataset. In our study, we randomly chose 14 patients with 539 slices as the training set and used the rest 6 patients with 256 slices for validation. All under-sampled MR images were created with a universal sampling pattern.

2.2. MTANN deep learning

In the field of image processing, supervised nonlinear image-processing techniques based on an artificial neural network (ANN), called a "neural filter" and a "neural edge enhancer," [17] have been investigated for the reduction of the quantum mottle in angiograms and supervised semantic segmentation of the left ventricles in angiography [18], respectively. By extending the neural filter and edge enhancer, MTANNs have been developed to accommodate the task of reduction of false positives in computerized detection of lung nodules in low-dose computed tomography (CT) [19]. MTANN has also shown promising performance in image processing, such as suppressing ribs in chest radiographs [20]. In this study, we aimed to remove truncation artifacts and improve image quality in under-sampled MR images.

The MTANN employs neural network regression in a convolution manner. Figure 1 illustrates the training phase of our MTANN technique for reducing artifacts in fast acquisition MRI. Our MTANN is trained with input under-sampled MR images together with the corresponding teaching fully-sampled images. Through the training, our MTANN learns the relationship between the input under-sampled MR images and the teaching fully-sampled MR images. Our MTANN deep learning model consists of an input layer, a convolutional layer, multiple fully-connected hidden layers, and an output layer. After training, the MTANN deep learning model is expected to output values close to the desired pixel value in fully-sampled teaching images.

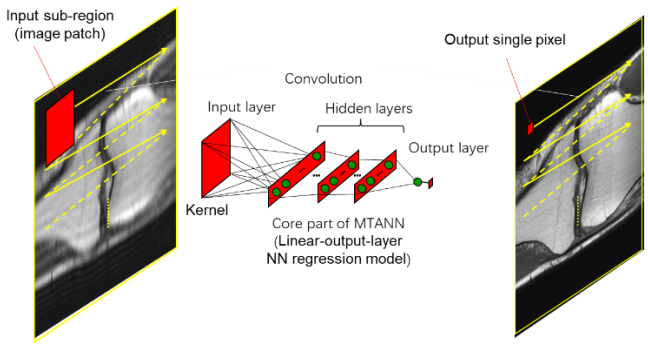

Fig. 1. The training phase of the proposed MTANN model for reducing artifacts in fast acquisition MRI. (a) Input under-sampled MR image; (b) supervised MTANN; (c) teaching fully-sampled MR image.

2.3. Sampling-Specific MTANN kernel

An advantage of our MTANN deep learning is that the shape of the MTANN convolution kernel can be designed with fewer limitations. We proposed k-space-sampling-pattern-specific kernel selection to fully exploit this advantage by considering the theoretical nature of the under-sampling process in the k-space. Figure 2 illustrates that the Fourier transform of the under-sampling pattern has non-zero values only in the center vertical line.

The convolution theorem suggests that with a specific under-sampling pattern, the corresponding under-sampled MR image can be regarded as a deteriorated fully-sampled image by applying the convolution operation with the Fourier transform this under-sampling pattern. As multiplication in the k-space is equal to convolution in the image domain, each pixel value in the under-sampled MR image is a linear combination of pixel values in the fully-sampled image located in the same vertical line. One specific under-sampling pattern uniquely determines the weight of this combination.

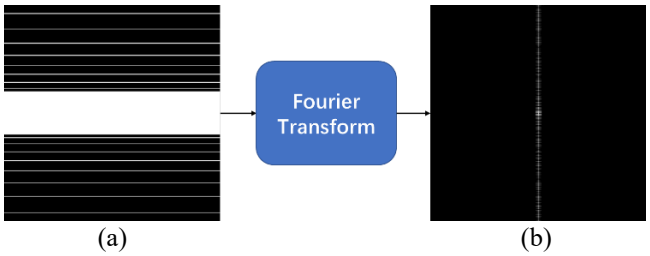

Fig.2. Fourier transform of the under-sampling pattern. (a) Under-sampling pattern; (b) Fourier transform of the under-sampling pattern has non-zero values only in the center vertical line.

Figure 3 illustrates an under-sampled test chart image. This example shows that truncation artifacts arise mostly near the horizontal high-contrast interfaces between bright and

dark regions, but almost no artifact appears near the vertical high-contrast interfaces between bright and dark regions.

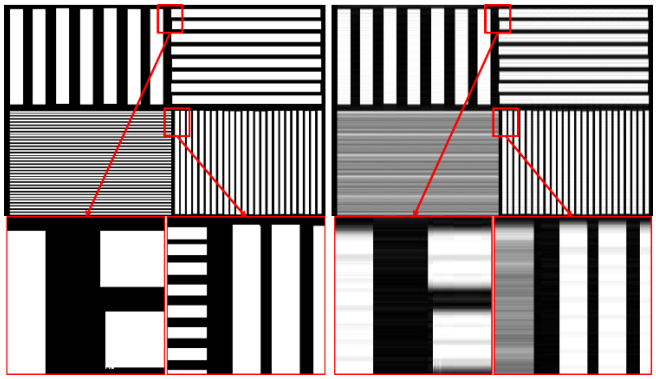

(a) (b)

Fig.3. Effects of under-sampling on the image quality of a test chart. (a) Test chart reconstructed from fully-sampled data; (b) Test chart reconstructed from under-sampled data. In the under-sampled test chart, artifacts and the degradation of image quality arise more near the horizontal high-contrast interfaces, but almost none near the vertical high-contrast interfaces.

This result suggests that a k-space-sampling-pattern-specific MTANN convolution kernel should include more pixels in the center vertical line to exploit more useful information for the prediction of fully-sampled images. We selected a convolution kernel among ones with different shapes to maximize the MTANN's performance. Figure 4 illustrates our special kernel for this problem, which has a balance between the vertical line and the local region near the center with a 29-pixels-length line and a 5 x 5 area, compared with a 7 x 7 ordinary square kernel. The number of non-zero elements in these two kernels is the same.

(a) (b)

Fig.4. (a) Our kernel for MTANN deep learning specific to the MR under-sampled data, which contains more pixels in the vertical direction. (b) Ordinary square kernel.

3. EXPERIMENTS AND RESULTS

An MTANN model was trained with simulated under-sampled MR data with a reduction factor of 4 as input and the corresponding fully-sampled MR data as "teaching" images in the image domain under the mean squared error (MSE) criterion. Through training, MTANN learned to convert under-sampled MR images to fully-sampled MR images, where artifacts were reduced substantially.

We used three-layered MTANN where the numbers of input, hidden, and output units were 49, 25, and 1. The learning rate was 0.001. With the hyper-parameters above, the training of the MTANN was performed 1,000,000 times and took about 90 minutes on a personal computer (Intel i7-8700K CPU, 3.2GHz with 32G RAM) with a GPU (GeForce GTX 1080, Nvidia). The execution time for the testing stage was 1.1 seconds per patient on average. With our MTANN technique, the image quality in the reconstructed MR images from under-sampled k-space data was substantially improved by reducing truncation artifacts while preserving anatomic structures

To evaluate the image quality quantitatively, we used the structural similarity index (SSIM), MSE, and the peak-signal-to-noise-ratio (PSNR) between the predicted MR images and fully-sampled MR images. The compressed sensing used a total variant regularizer. After the optimization of 200 iterations with around 162 seconds per case, it reached a PSNR of 34.9± 2.9dB, and an SSIM of 0.888 ± 0.042.

The proposed MTANN outperformed the compressed sensing method at a statistically significant level ($P<<0.05$ in paired t-tests) with a PSNR of 37.2 ± 2.3 dB and an SSIM of 0.937 ± 0.016. Figure 5 illustrates a comparison of a resultant MR image by our MTANN model with the results by the compressed sensing method. Artifacts (blue arrow) and loss of details (red arrow) were seen in compressed sensing images, whereas they were reduced substantially in our MTANN images. Table 1 represents a quantitative evaluation of the image quality of resultant MR images and execution time by the compressed sensing method and our MTANN model.

Tab. 2. Quantitative evaluation of the image quality and execution time of the resultant MR images by the compressed sensing method and our MTANN.

	Compressed sensing	MTANN with specific kernel
PSNR	34.9 ± 2.9	37.2 ± 2.3
MSE	22.5 ± 14.2	12.9 ± 6.3
SSIM	0.888 ± 0.042	0.937 ± 0.016
Execution Time(Sec.)	162 ± 11	1.10 ± 0.14

4. CONCLUSIONS

We have developed an image-processing technique based on our original supervised MTANN deep learning algorithm coupled with a k-space-sampling-pattern-specific kernel. Our technique learned to remove artifacts and recover image details in the under-sampled MR image.

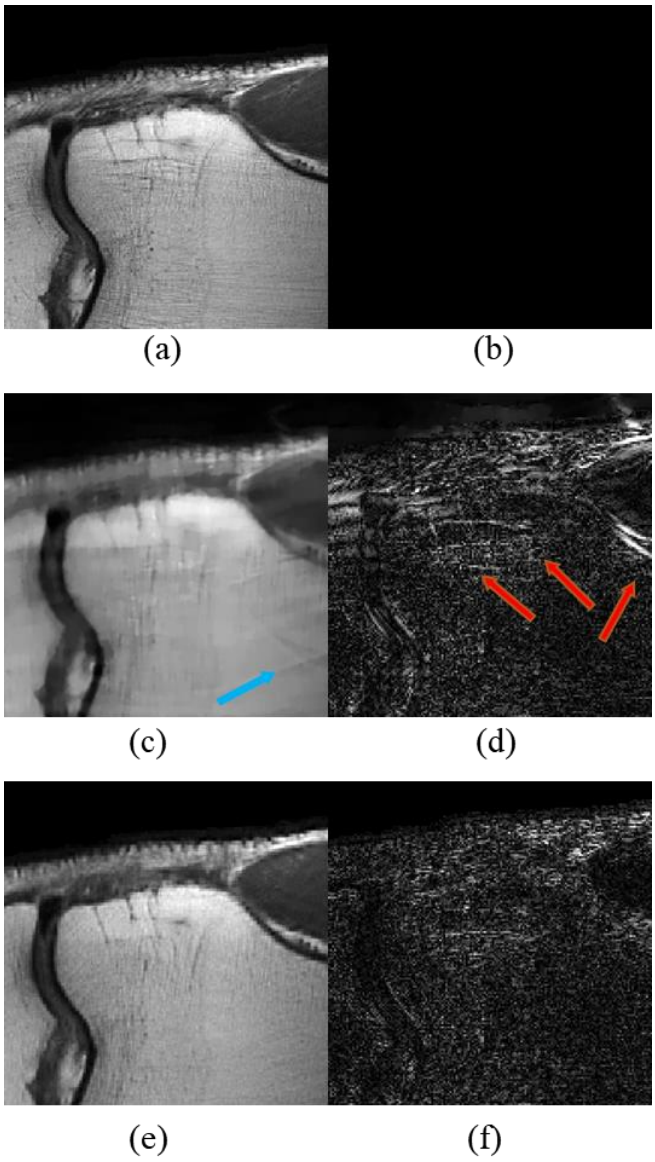

Fig. 5. Comparisons of our MTANN method with conventional methods. The images in the left and right columns are MR images and difference (error) maps between an MR image and the corresponding "gold-standard" fully-sampled MR image (a), respectively. (c), and (e) are the predicted images by the compressed sensing method and the proposed MTANN model, respectively. Significant artifacts (blue arrows) are seen in the resultant images by the compressed sensing methods. The difference maps indicate the loss of details (red arrows) in the compressed sensing images.

The performance measured by PSNR, MSE, and SSIM of MTANN deep learning was superior to those of the compressed sensing methods at a statistically significant level. The proposed MTANN technique improved the image quality by reducing artifacts substantially in 4-times faster acquisition MRI. Reduction in acquisition time by 75% in MRI would be beneficial for patients as well as radiologists, which improves the throughput of MR exams.

5. ACKNOWLEDGMENTS

This work was supported in part by a JST-Mirai Program Grant. The authors are grateful to the members of the Suzuki Lab for their valuable discussions.

6. REFERENCES

[1] D. I. Hoult and B. Bhakar, "NMR signal reception: Virtual photons and coherent spontaneous emission," *Concepts Magn. Reson.*, vol. 9, no. 5, pp. 277–297, 1997.
[2] M. Lustig and J. M. Pauly, "SPIRiT: Iterative self-consistent parallel imaging reconstruction from arbitrary k-space," *Magn. Reson. Med.*, vol. 64, no. 2, pp. 457–471, 2010.
[3] S. Ljunggren, "Imaging methods," *J. Magn. Reson.*, vol. 54, pp. 338–343, 1983.
[4] E. Pusey *et al.*, "Magnetic resonance imaging artifacts: mechanism and clinical significance.," *Radiographics*, vol. 6, no. 5, pp. 891–911, 1986.
[5] M. Lustig, D. L. Donoho, J. M. Santos, and J. M. Pauly, "Compressed Sensing MRI," *IEEE Signal Process. Mag.*, vol. 25, no. 2, pp. 72–82, 2008.
[6] S. Ma, W. Yin, Y. Zhang, and A. Chakraborty, "An efficient algorithm for compressed MR imaging using total variation and wavelets," *26th IEEE Conf. Comput. Vis. Pattern Recognition, CVPR*, 2008.
[7] J. P. Haldar, D. Hernando, and Z. P. Liang, "Compressed-sensing MRI with random encoding," *IEEE Trans. Med. Imaging*, vol. 30, no. 4, pp. 893–903, 2011.
[8] M. Lustig, D. Donoho, and J. M. Pauly, "Sparse MRI: The application of compressed sensing for rapid MR imaging," *Magn. Reson. Med.*, vol. 58, no. 6, pp. 1182–1195, 2007.
[9] K. Suzuki, "Overview of deep learning in medical imaging," *Radiol. Phys. Technol.*, vol. 10, no. 3, pp. 257–273, 2017.
[10] K. Suzuki, J. Liu, A. Zarshenas, T. Higaki, W. Fukumoto, and K. Awai, "Neural Network Convolution (NNC) for Converting Ultra-Low-Dose to ``Virtual'' High-Dose CT Images," in *Machine Learning in Medical Imaging*, 2017, pp. 334–343.
[11] K. Suzuki, and R. Smathers, "Radiation Dose Reduction in Full-field Digital Mammography (FFDM) by Means of Pixel-based Trainable Nonlinear Regression (PTNR)," Program of RSNA, PH259-SD-TUB9, 2015.
[12] J. Liu *et al.*, "Radiation dose reduction in digital breast tomosynthesis (DBT) by means of deep-learning-based supervised image processing," in *Medical Imaging 2018: Image Processing*, 2018, vol. 10574, p. 105740F.
[13] P. Wang, E. Z. Chen, T. Chen, V. M. Patel, and S. Sun, "Pyramid Convolutional RNN for MRI Reconstruction," 2019.
[14] J. Zbontar *et al.*, "fastMRI: An Open Dataset and Benchmarks for Accelerated MRI," pp. 1–35, 2018.
[15] K. Hammernik *et al.*, "Learning a variational network for reconstruction of accelerated MRI data," *Magn. Reson. Med.*, vol. 79, no. 6, pp. 3055–3071, 2018.
[16] O. Ronneberger, P. Fischer, and T. Brox, "U-net: Convolutional networks for biomedical image segmentation," *Lect. Notes Comput. Sci.* vol. 9351, pp. 234–241, 2015.
[17] K. Suzuki, I. Horiba, and N. Sugie, "Neural Edge Enhancer for Supervised Edge Enhancement from Noisy Images," *IEEE Trans. Pattern Anal. Mach. Intell.*, vol. 25, no. 12, pp. 1582–1596, 2003.
[18] K. Suzuki, I. Horiba, N. Sugie, and M. Nanki, "Neural filter with selection of input features and its application to image quality improvement of medical image sequences," *IEICE Trans. Inf. Syst.*, vol. E85-D, no. 10, pp. 1710–1718, 2002.
[19] K. Suzuki, I. Horiba, N. Sugie, and M. Nanki, "Extraction of Left Ventricular Contours From Left Ventriculograms by Means of a Neural Edge Detector," *IEEE Trans. Med. Imaging*, vol. 23, no. 3, pp. 330–339, 2004.
[20] K. Suzuki, H. Abe, H. MacMahon, and K. Doi, "Image-processing technique for suppressing ribs in chest radiographs by means of massive training artificial neural network (MTANN)," *IEEE Trans. Med. Imaging*, vol. 25, no. 4, pp. 406–416, 2006.

7. COMPLIANCE WITH ETHICAL STANDARDS

Ethical approval was not required because of the retrospective use of the open source data [15].